

## Accuracy of a Finite-Difference Method for Computing Lake Currents\*

JOHN R. BENNETT † AND JOAN E. CAMPBELL

*Great Lakes Environmental Research Laboratory,  
U.S. Department of Commerce,  
2300 Washtenaw Avenue, Ann Arbor, Michigan 48104*

Received March 25, 1985; revised March 25, 1986

A semi-analytic model is used to assess the accuracy of a finite-difference model for computing lake currents. Both models solve the vorticity equation for two-dimensional, time-dependent flow to compute currents in a circular lake with a parabolic depth profile. The semi-analytic solution is obtained by using separation of variables to remove the azimuthal dependence and reduce the equations in cylindrical coordinates to a single equation in two variables, time and radius. This equation is then solved by a finite-difference technique for grid sizes small enough that the solution appears to converge. Comparison with the rectangular finite-difference solution shows a strong improvement in accuracy with decreasing grid size. It is found that about 20 grid points across a lake basin are required to adequately resolve wind-driven flow. © 1987 Academic Press, Inc.

### 1. INTRODUCTION

One of the major uses of the numerical calculation of fluid flow is the understanding of flow subject to time dependent forcing in complex geometries. However, the accuracy of these calculations is usually estimated by comparison with solutions for very simple flows which can be calculated by analytical methods. For example, there is a large body of literature on the accuracy of methods for solving the one-dimensional advection equation in an infinite domain, but very few papers on two-dimensional accuracy tests. The reason for this gap is that it is difficult to find exact solutions for complex flows.

One way to combat the lack of exact solutions is to develop combined analytical and numerical methods which generate approximate, but not closed form solutions. This paper uses this method to assess the accuracy of a lake circulation model. The most relevant exact solutions are those of Lamb [8] and Ball [12]; however, these are limited to frictionless flow in a basin which has zero depth at the shore—a very difficult numerical problem and not very relevant to practical models.

\* GLERL Contribution No. 366.

† Current address: Environmental Research Institute of Michigan, P.O. Box 8618, Ann Arbor, Mich. 48107.

The semi-analytical method used here is fairly elaborate because it was originally developed to study the dynamics of lake circulation; i.e., it is a lake circulation model in its own right. This model was used in [1] to study the nonlinear effects of the large thermocline displacements and currents observed in Lake Ontario and in [2] to study the general problem of wave rectification in lakes and to apply it to Lake Kinneret (the Sea of Galilee). In these papers a two-layer model was carried out to second order in amplitude. In the first paper, the model was driven by observed winds; in the second it was driven by periodic winds to simulate the very regular observed diurnal pattern of wind forcing.

One of the conclusions of the Lake Ontario study was that grid resolution was very important. For poor resolution, the nonlinear terms were underestimated; this was particularly true near the coast, where the currents and thermocline displacements were greatest.

To isolate the role of grid resolution in a barotropic rigid lid model we use a reduced version of the equations; nonlinear terms and the density variations are ignored. The major source of numerical error in it is the approximation of the coast by a finite-difference grid.

It is of practical importance to understand the errors in this simple model because it is used in the realtime prediction of currents and spill trajectories in the Great Lakes [3]. The accuracy of the model must be weighed against the uncertainties in the driving forces, the uncertainties in the initial positions of spills or wrecks, and the need for fast response.

## 2. THE LAKE CIRCULATION MODEL

The most fundamental model assumption is that the water is homogeneous. This limits the applicability of the model since currents driven by density gradients can be a significant factor in determining the circulation patterns. Density driven currents are most common in the Great Lakes during the spring and summer months when there are large vertical and horizontal temperature gradients.

Momentum advection and lateral friction are assumed to be negligible. According to [1] and [2], momentum advection is more important during the stratified period and its effects are usually less important in the short simulations required by the operational model. The consequence of neglecting lateral friction is that, at the shore, only the normal component of velocity is zero. This is a reasonable assumption because for the shoreline depths used here the observed longshore current speeds are high.

For all the calculations in this paper, a Coriolis parameter of  $10^{-4} \text{ s}^{-1}$ , a value typical of mid-latitudes, was used. The time step used is 1 h, a value low enough that there are no significant time stepping errors. The time step limit for computational stability is proportional to  $f^{-1}$ ; its exact magnitude depends on the normal mode frequencies of the system. The exact solution of the normal modes of an

elliptic paraboloid given in Lamb [8] shows that the minimum period is  $6\pi/f$ . With the above values of  $f$  and  $\Delta t$ , there are at least 50 time steps per period.

The shape and bathymetry of the lake is represented by an array of square grid boxes. For the circular paraboloid model lake (Fig. 1), a bathymetric grid was generated for three grid sizes: 10, 5, and 2.5 km. These values correspond to 10, 20, and 40 grid points across the diameter. An elementary grid box and the outline of the three grids is given in Fig. 2. Water depth is defined at the center of the grid box, the  $x$ -component of transport ( $U$ ) is defined at the center of the east and west sides, and the  $y$ -component of transport ( $V$ ) is defined at the center of the north and south sides. The stream function is defined at the corners of each box. The depth is also linearly interpolated to the corners where necessary.

In the operational model, the rigid-lid approximation is used for three reasons. First, the currents in the gravitational oscillations filtered out by it are weak in most areas of the Great Lakes. Second, because a large time step can be used, it requires less computer time. Third, for low frequency currents, the effects of the Earth's rotation are calculated more accurately. The reason for this is that in free surface models using the staggered grid employed here, the Coriolis terms must be averaged over four grid points. When these equations are analyzed in the limit of large values of gravity, it can be shown that this is equivalent to approximating the Jacobian derived below by Arakawa's [4] finite-difference formula labeled  $J_3$ . Bennett and Schwab [5] showed that this formula is not accurate; it even allows some waves to travel in the wrong direction.

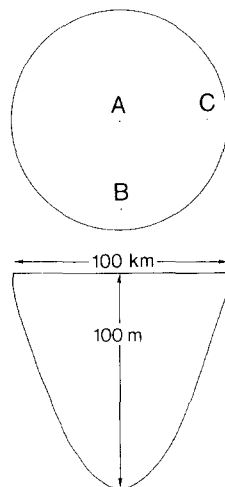


FIG. 1. Plan and cross section views of a circular paraboloid lake. A, B, and C are the locations of the transports plotted in Fig. 4.

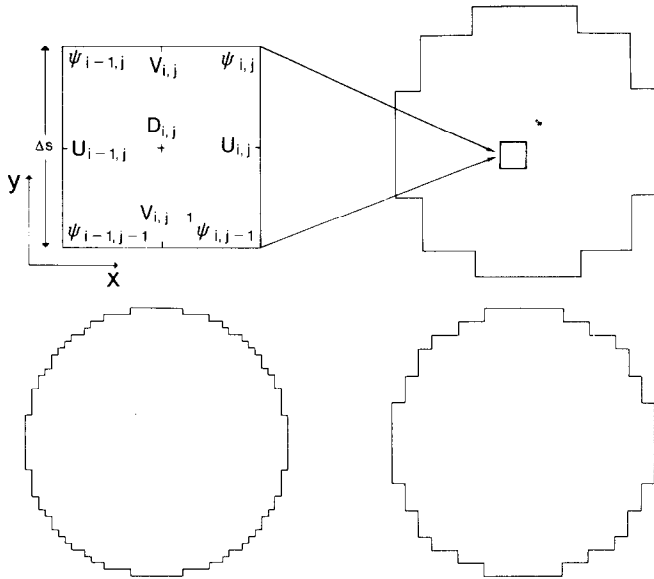


FIG. 2. Pictorial representation of the grid box and lake outlines for each of three grid sizes: 10, 5, and 2.5 km. Water depth ( $D$ ) is defined at the center of the grid box, the  $x$ -component of transport ( $U$ ) is defined at the center of the right side, and the  $y$ -component of transport ( $V$ ) is at the center of the top. Stream function ( $\psi$ ) is defined at the corners.

With this approximation, conservation of mass requires the flow to be non-divergent,

$$\frac{\partial U}{\partial x} + \frac{\partial V}{\partial y} = 0, \tag{1}$$

where  $U = \int_0^D u \, dz$  and  $V = \int_0^D v \, dz$  are the depth-integrated currents—the mass transports. This constraint allows the two transport components to be expressed in terms of a single variable,  $\psi$ , the stream function. The transports are then

$$U = \frac{-\partial\psi}{\partial y}, \quad V = \frac{\partial\psi}{\partial x}. \tag{2}$$

A further consequence of the rigid-lid approximation is that the two momentum equations [1] can be combined into a single equation for  $\psi$ ,

$$\frac{\partial}{\partial t} (\nabla \cdot D^{-1} \nabla \psi) + fJ(\psi, D^{-1}) = \frac{\partial}{\partial x} \frac{\tau_y^s - \tau_y^B}{\rho D} - \frac{\partial}{\partial y} \frac{\tau_x^s - \tau_x^B}{\rho D}, \tag{3}$$

where

$$J(\psi, D^{-1}) = \frac{\partial\psi}{\partial x} \frac{\partial D^{-1}}{\partial y} - \frac{\partial\psi}{\partial y} \frac{\partial D^{-1}}{\partial x} \tag{4}$$

is the Jacobian of the inverse depth and the stream function.

In this equation for  $\psi$ ,  $D$  is the depth;  $f$  is the Coriolis parameter ( $f = 2\Omega \sin \phi$ , where  $\Omega$  is the angular speed of rotation of the earth and  $\phi$  is the latitude);  $\rho$  is water density (assumed uniform);  $\tau_x^s, \tau_y^s$  are the  $x, y$  components of the wind stress vector; and  $\tau_x^b, \tau_y^b$  are the  $x, y$  components of the bottom stress vector. The boundary condition is that there be no transport normal to the shoreline; thus  $\psi$  is set equal to zero there.

The prediction equation for the stream function is

$$\frac{V \cdot D^{-1} \nabla \psi^{n+1} - \nabla \cdot D^{-1} \nabla \psi^n}{\Delta t} + fJ(\psi^n, D^{-1}) = \frac{\partial}{\partial x} \frac{\tau_y^s}{\rho D} - \frac{\partial}{\partial y} \frac{\tau_x^s}{\rho D} - \frac{C_d}{\rho} \cdot SPD \cdot \left( \frac{\partial \bar{V}^n}{\partial x D^2} - \frac{\partial \bar{U}^n}{\partial y D^2} \right), \tag{5}$$

where the operator

$$(-^n) = \frac{(\ )^{n+1} + (\ )^n}{2}.$$

$C_d$  is the drag coefficient and  $SPD$  is the average current speed. The values of  $C_d$  and  $SPD$  were taken to be 0.002 and 0.10 ms<sup>-1</sup>, respectively. The time differencing in the above equation follows the trapezoidal rule and results in an implicit representation of  $\psi^{n+1}$ . This does not increase the computational work since the solution can be combined with the relaxation procedure required to convert vorticity to streamfunction. In this equation, the vorticity and transport components are evaluated with elementary second-order difference formulas, with appropriate two-point averages to compute  $D^{-1}$  at points other than at stream function points. The Jacobian, term is evaluated according to Arakawa [4] method number  $J_7$  as follows:

$$\begin{aligned} \Delta s J(\psi, D^{-1}) &= \psi_{i+1,j}(D_{i,j+1}^{-1} + D_{i+1,j+1}^{-1} - D_{i,j-1}^{-1} - D_{i+1,j-1}^{-1}) \\ &\quad + \psi_{i-1,j}(-D_{i,j+1}^{-1} - D_{i-1,j+1}^{-1} + D_{i,j-1}^{-1} + D_{i-1,j-1}^{-1}) \\ &\quad + \psi_{i,j+1}(-D_{i+1,j}^{-1} - D_{i+1,j+1}^{-1} + D_{i-1,j}^{-1} + D_{i-1,j+1}^{-1}) \\ &\quad + \psi_{i,j-1}(D_{i+1,j}^{-1} + D_{i+1,j-1}^{-1} - D_{i-1,j}^{-1} - D_{i-1,j-1}^{-1}) \\ &\quad + \psi_{i+1,j+1}(-D_{i+1,j}^{-1} + D_{i,j+1}^{-1}) + \psi_{i+1,j-1}(D_{i+1,j}^{-1} - D_{i,j-1}^{-1}) \\ &\quad + \psi_{i-1,j+1}(-D_{i-1,j}^{-1} - D_{i,j+1}^{-1}) + \psi_{i-1,j-1}(-D_{i-1,j}^{-1} + D_{i,j-1}^{-1}). \end{aligned} \tag{6}$$

Further details of this model and the computer programs are documented in [6].

In order to isolate the effects of grid resolution in this model, we have held the potential effects of other variables to a minimum. To do so, we have chosen to apply a uniform wind stress. A constant wind stress of 0.1 nt m<sup>-2</sup> from the west was

applied for a period of 1 day. For the next 4 days, the wind stress was zero. This wind stress pattern is representative of a typical Great Lakes storm.

In Fig. 3a the stream function patterns for the finest gridsize are plotted every 6 h for the first day, during which the wind stress was  $0.1 \text{ nt m}^{-2}$  from the west (left). Initially, the flow agrees with Bennett's theory [7]. The flow is aligned with the wind, the shallow water going in the direction of the wind and the deep water moving in the opposite direction; the magnitude increases linearly with time. Thus, there is one clockwise gyre and one counterclockwise gyre, a pattern that persists throughout the complete simulation. The effect of the Coriolis force is to cause the gyres to move counterclockwise around the basin in the manner of the normal modes of a circular paraboloid given in [8, Sect. 212].

In Fig. 3b the stream function patterns are plotted every day for 4 days after the wind stress is set to zero. The flow magnitude immediately begins to decrease from the maximum reached at 1 day. Because the friction term is more significant in the shallow water, the gradient decreases faster there than in the deep water. In addition, the gyres continue to travel counterclockwise around the shore as they decay. The period of this free motion agrees with the theoretical value for the fundamental mode from [8] of 5.1 days. This solution is very realistic. Analytical models similar to this have been used to interpret observations in Lake Ontario [9] and Lake Michigan [10]. In addition, Schwab [11] has run the numerical model used here with realistic Lake Michigan topography and observed winds and found that computed current fluctuations agree well with observed current fluctuations in the 1- 10-day period range.

### 3. ACCURACY OF THE CIRCULATION MODEL

A model using the same assumptions was used to calculate a more rigorous numerically convergent solution. Assuming  $D$  is independent of the azimuthal coordinate,  $\theta$ , Eq. (3) in cylindrical coordinates is

$$\frac{\partial Z}{\partial t} + \frac{f}{D^2} \frac{\partial D}{\partial r} \frac{\partial \psi}{\partial \theta} = \frac{\partial}{\partial r} \frac{r \tau_\theta}{D} - \frac{\partial}{\partial \theta} \frac{\tau_r}{D} - \alpha \left( \frac{\partial}{\partial r} \frac{r}{D^2} \frac{\partial \psi}{\partial r} + \frac{1}{r D^2} \frac{\partial^2 \psi}{\partial \theta^2} \right), \tag{8}$$

where

$$Z = \frac{\partial}{\partial r} \frac{r}{D} \frac{\partial \psi}{\partial r} + \frac{1}{r D} \frac{\partial^2 \psi}{\partial \theta^2}. \tag{9}$$

Because the equation is linear and the wind stress is uniform, Eq. (8) can be simplified by separation of variables and  $\psi$  can be written

$$\psi(r, \theta, t) = \psi_c(r, t) \cos \theta + i \psi_s(r, t) \sin \theta. \tag{10}$$

Substitution of this expression into Eqs. (8) and (9) and application of the

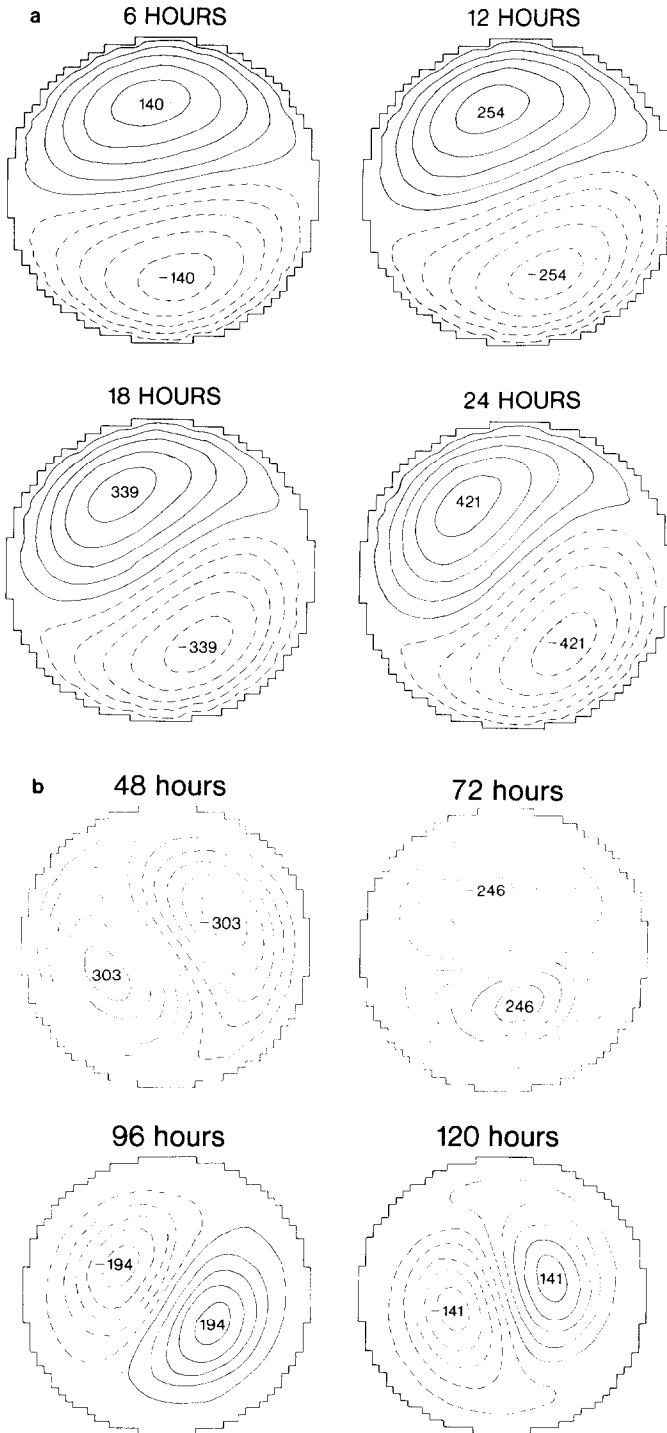


FIG. 3. (a) Stream function patterns every 6 h for the first day, during which the wind stress was from the west (left). Solid lines represent counterclockwise flow; dashed lines indicate clockwise flow. (b) Stream function patterns every day for 4 days after the wind stress is set to zero.

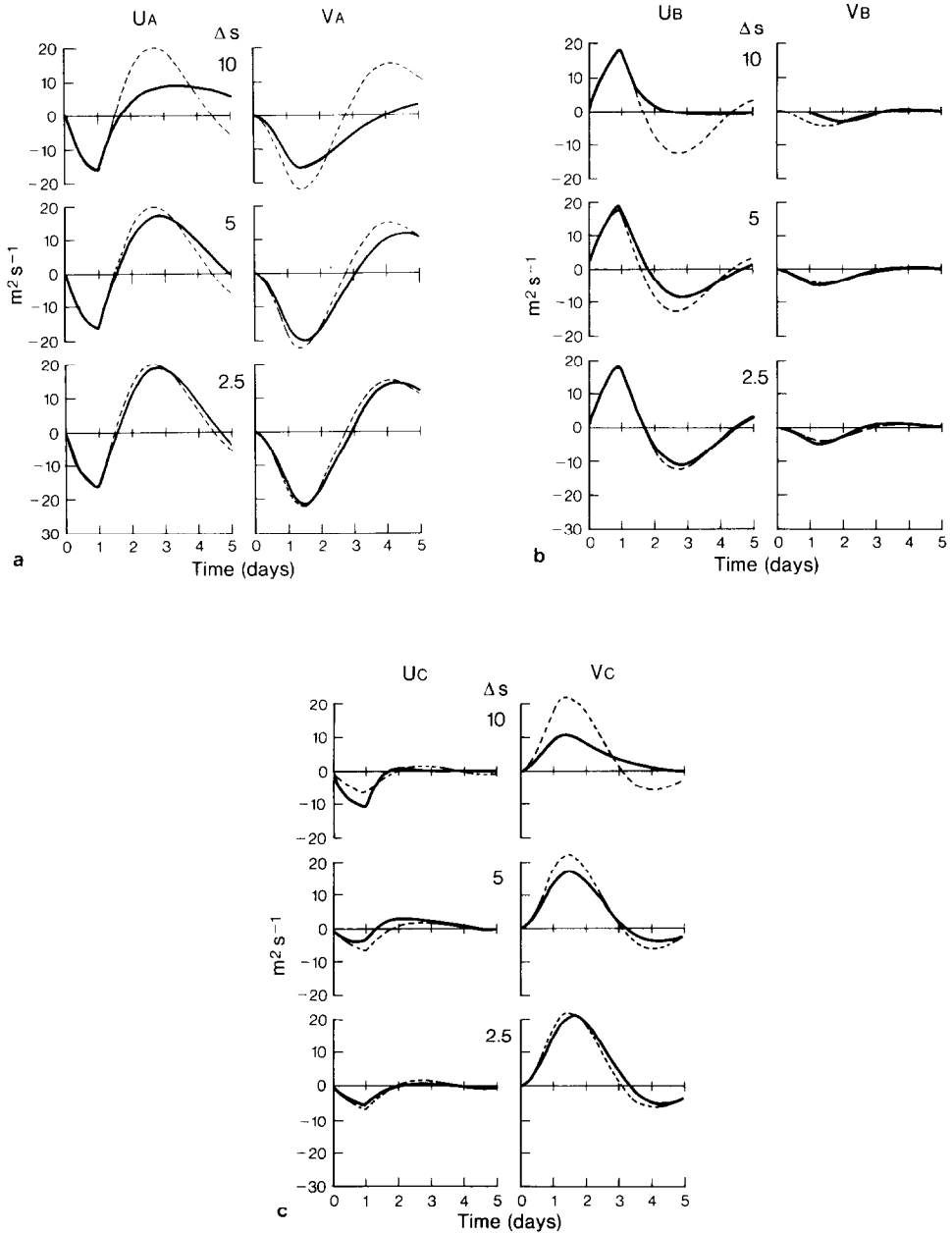


FIG. 4. (1-c) Solutions for eastward ( $U$ ) and northward ( $V$ ) transport for three locations (labelled A, B, and C in Fig. 1) compared to semi-analytical solutions for three grid resolutions (10, 5, and 2.5 km). Dashed line is the exact solution. Solid line is the finite-difference solution.



trapezoidal rule for time differencing yield a complex tridiagonal matrix equation for the variable  $\psi_c + i\psi_s$ . This equation is diagonally dominant as long as the quantity  $f \cdot \Delta t$  is small and is solved by the standard tridiagonal algorithm. As stated earlier,  $\Delta t$  is 1 h for all calculations and time differencing errors were negligible.

Solutions were calculated for grid sizes of 10, 5, 2.5, and 1.25 km (10, 20, 40, and 80 grid points per diameter). Since the last three solutions for  $\psi$  and its radial derivatives are nearly identical, we conclude that the method has converged and that the solution is accurate.

After varying only the grid resolution of the bathymetry used as input to the finite difference model, the solutions for eastward and northward transport were compared to the accurate solution. Results of this comparison are shown in Fig. 4 at the locations labelled A, B, and C in Fig. 1.

The low-resolution (10 km) grid solution compares favorably to the accurate solution only for the first day, during wind stress. After the first day, the 10-km-grid solution decays much more rapidly than it should. The natural period appears to be much longer since the gyres do not respond as rapidly as they should. Even in the middle of the lake, the stream function values of the solution do not match those of the accurate solution. The 10-km grid solution is not very accurate. The 5-km grid solution is considerably better, and the 2.5-km grid resolution is closer to an exact fit.

#### 4. SUMMARY

The objective of this paper was to assess the accuracy of a finite-difference technique for computing lake currents. To do so the currents in a 100-km-diameter lake of parabolic depth profile were calculated for three different grid sizes (10, 5, and 2.5 km). The simulated time span was 5 days with a uniform wind stress being applied for only the first day. The solutions for this test case were compared to a numerically convergent solution from a model using the same physical assumptions. The effects of the grid size became most apparent after the wind stress had been removed and the general two-gyre circulation pattern began to oscillate and decay. The 10-km grid (10 grid points per diameter) solution was poor, the 5-km (20 grid points per diameter) solution acceptable, and the 2.5-km (40 grid points per diameter) solution was not significantly different from the accurate solution. Thus, at least 20 grid points are required across a lake basin to adequately resolve wind driven flow in a homogeneous model of the dimensions of the Great Lakes.

#### REFERENCES

1. J. R. BENNETT, *J. Phys. Oceanogr.* **8** 1095, (1978)
2. H. W. OU AND J. R. BENNETT, *J. Phys. Oceanogr.* **9** 1112, (1979).
3. D. J. SCHWAB, J. R. BENNETT, AND E. W. LYNN, NOAA Tech. Memo., No. ERL GLERL-53, 1984 (unpublished).

4. A. ARAKAWA, *Proc. Am. Math. Soc.* **24**, (1970).
5. J. R. BENNETT AND D. J. SCHWAB, *J. Comput Phys.* **44** 359, (1981).
6. D. J. SCHWAB, J. R. BENNETT, AND A. T. JESSUP, NOAA Tech. Memo., No. ERL-GLERL-38, 1981 (unpublished).
7. J. R. BENNETT, *J. Phys. Oceanogr.* **4** 400, (1974).
8. H. LAMB, *Hydrodynamics*, 6th ed. (Cambridge Univ. Press, Cambridge, 1932).
9. G. E. BIRCHFIELD AND B. P. HICKIE, *J. Phys. Oceanogr.* **7** 691, (1977).
10. J. H. SAYLOR, J. C. K. HUANG, AND R. O. REID, *J. Phys. Oceanogr.* **10**, 1814 (1980).
11. D. J. SCHWAB, *J. Phys. Oceanogr.* **13** 2213, (1983).
12. F. K. BALL, *J. Fluid Mech.* **23** 545, (1965).